

MAGNETIC FILMS OF TECHNICAL INTEREST PREPARED BY PULSED LASER DEPOSITION

J. M. Barandiarán*, M. L. Fdez-Gubieda, J. Gutiérrez, I. Orúe, A. García Arribas, G. V. Kurlyandskaya^a

Departamento de Electricidad y Electrónica, Facultad de Ciencia y Tecnología
Universidad del País Vasco, UPV/EHU, P.O. Box 644, 48080, BILBAO, Spain

^aPresent address: Departamento de Física, Facultad de Ciencias, Universidad de Oviedo, Calvo Sotelo s/n 33007, Oviedo, Asturias, Spain

Magnetic thin films are very interesting materials for applications in electronics, sensors and other fields where miniaturisation is a key issue. The great variety of compositions, structures and magnetic features makes it difficult to provide a single method of preparation for all of them. Pulsed laser deposition (PLD) has many advantages in this sense. It can be used for oxides and metals, epitaxial growth and amorphous film preparation, and a great number of parameters can be independently controlled during deposition. In this work we summarise recent research on magnetic thin films obtained by PLD, including METGLASS like amorphous films for magnetoelastic or Giant Magneto-impedance applications, nano-granular Co-Cu and Fe-Ag alloys with Giant Magneto-resistance and mixed oxides with perovskite structure and Colossal Magneto-resistance. The preparation conditions and magnetic and magneto-transport properties are discussed.

(Received April 26, 2004; accepted June 3, 2004)

Keywords: Magnetic thin films, Laser deposition, Magnetic sensors

1. Introduction

Technology for the preparation of magnetic materials in thin film shape has evolved considerably over recent years. Amorphous thin films have interesting magnetic, magnetoelastic and magnetotransport properties suitable for many technological applications [1-5]. Various techniques can be used to prepare thin films, multilayers and more complicated nanostructures such as electrodeposition [5-6], molecular beam epitaxy and rf-sputtering [7-12]. Preparation of soft magnetic amorphous thin films and granular films by pulsed laser deposition (PLD) has recently been reported [13-15]. This method was also used in former Colossal Magneto-resistance studies in oxides for epitaxial growth of doped manganites [16,17].

Laser ablation is fast, relatively simple and therefore suitable for films preparation of all kind of materials. At the same time, the properties of thin films prepared by pulsed laser deposition depend on many available parameters that must be taken into account in order to achieve the desired magnetic properties. In laser deposition important parameters are: the revolution speed of the target, the beam energy density, the distance between the target and the substrate, the substrate composition structure and temperature and the atmosphere in the chamber during deposition. For example at small distances the deposition rate is higher because of the higher concentration of the evaporated components. By contrast, at short distances with laser fluences above 5 J/cm², an effect opposite to deposition occurs, the process known as re-sputtering, which results in more homogeneous film formation [14]. At high fluences the sprinkle effect can be a key feature for depositing at short distances.

* Corresponding author: manub@we.lc.ehu.es

In this work we review recent studies of the magnetic properties laser ablated thin films prepared by controlling the different parameters mentioned, in order to obtain films which are suitable for sensor applications.

2. Experimental methods

Thin films were prepared using a $\lambda=248$ nm wavelength KrF excimer laser delivering 30 ns pulses and operating at 1-20 Hz repetition rate. The energy per pulse can reach 300 mJ. The geometry of the experimental set-up is shown in Fig. 1, and the general view in Fig. 2. The laser beam is focused by means of a quartz lens and window onto the target, which is located inside the vacuum chamber. The chamber can be evacuated to 10^{-6} mbar by means of a turbo molecular pump. For oxide deposition the chamber is maintained at a given oxygen pressure by means of an electrical valve operated in a feedback loop. The target can be rotated at angular speeds between 0 and 300 r.p.m. The ablated material forms a "plume" and deposits on a substrate located opposite the target. The distance between the target and the substrate can be changed between 30 and 60 mm. Different substrates can be mounted in a heated stage able to reach temperatures up to 800°C. A metallic mask is used to reduce the deposit to a circle of 15 mm in diameter as to maintain the maximum homogeneity in composition and thickness.

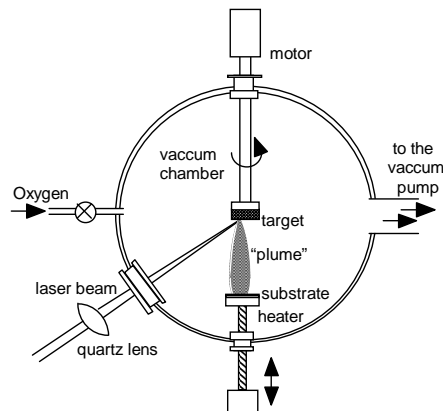


Fig. 1. Scheme of the PLD set-up.

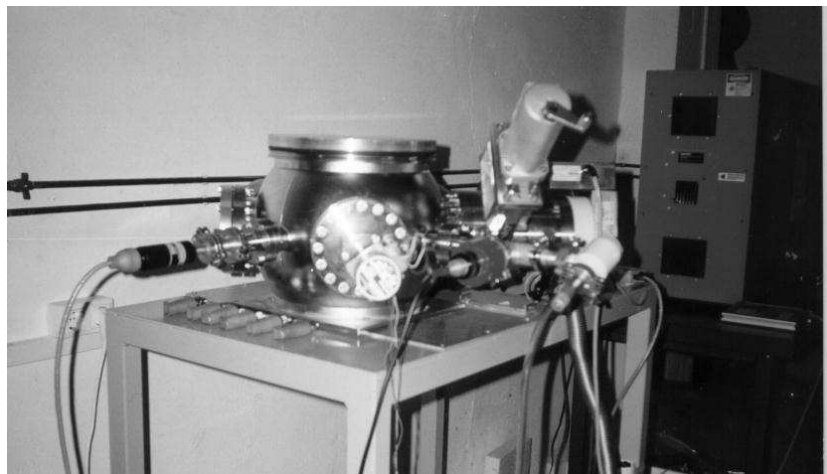


Fig. 2. A general view of the PLD apparatus.

The samples were examined by means of X-ray diffraction, profilometry, magnetic and electric resistivity measurements and, in some cases, by Atomic Force Microscopy. Most of the films were metallic either amorphous or crystalline, and the absence of oxides was carefully

checked. In oxide films, the correct structure and the polycrystalline or epitaxial character of the films is easy to ascertain from X-ray diffraction. Magnetisation curves were measured by induction or magneoptical Kerr effect (MOKE) methods. For induction, a hysteresis loop tracer operating at a frequency of 50 Hz or a SQUID magnetometer was used. MOKE was performed in a longitudinal geometry by means of a modulated semiconductor laser and lock-in detection. The details of similar devices for inductive and MOKE measurements are easily found in the literature [18,19].

3. Amorphous magnetostrictive films

The amorphous ferromagnetic alloys are ideal candidates for magnetoelastic applications. Because of their amorphous structure they show negligible magnetic anisotropy and, even with moderate magnetostriction constants, they can have a extremely high sensitivity to applied stresses. Typical compositions of relatively large magnetostriction are Fe rich ones, and specially those including about 25% Co as metallic component. One of those is the well known $\text{Fe}_{67}\text{Co}_{18}\text{B}_{14}\text{Si}_1$ available from Honeywell as METGLAS 2605Co[®]. Its magnetostriction constant is about 35 ppm. Among the different preparation parameters the fluence of the laser beam can be critical for the production of soft amorphous magnetic thin films. This is because of the possible formation of a non-homogeneous structure with crystalline clusters embedded into the amorphous matrix, and the appearance of large internal stresses during the deposition process.

All depositions of amorphous alloys were performed in a vacuum chamber evacuated at a pressure of 10^{-6} mbar. Amorphous METGLAS 2605Co[®] ($\text{Fe}_{67}\text{Co}_{18}\text{B}_{14}\text{Si}_1$) ribbons were used as a target, rotating with a frequency of 2.5 Hz. The samples were deposited at room temperature onto boro-silicate glass substrates specially tested by atomic force microscopy to control the roughness [20]. Circular films of 15 mm diameter assure homogeneity and isotropy of the demagnetising field. We used two different regimes of deposition. First (regime 1) with the laser beam focused on the target [21]. The distance between the target and the substrate was 50 mm, and the fluency 5 J/cm^2 . In this case the thickness of the film increases linearly with the deposition time. In another set of samples (regime 2), the position of the focusing lens, relative to the target, was changed. The deposition time was fixed at 30 min, the distance between the substrate and the target, d , was kept at 35 mm and a lower fluency of 4 J/cm^2 was used in order to avoid the sprinkle effect and the creation of crystalline phases.

The structure of the films was analysed by X-ray diffraction using $\text{Cu K}\alpha$ radiation. Fig. 3 shows the X-ray diffraction pattern of FeCoBSi films deposited at a distance of 35 mm for an in-focus regime. The structure is fully amorphous for fluences below 5 J/cm^2 . Fluences higher than $8\text{-}10 \text{ J/cm}^2$ resulted in crystalline films, but other parameters have also great influence on the magnetic properties of the films.

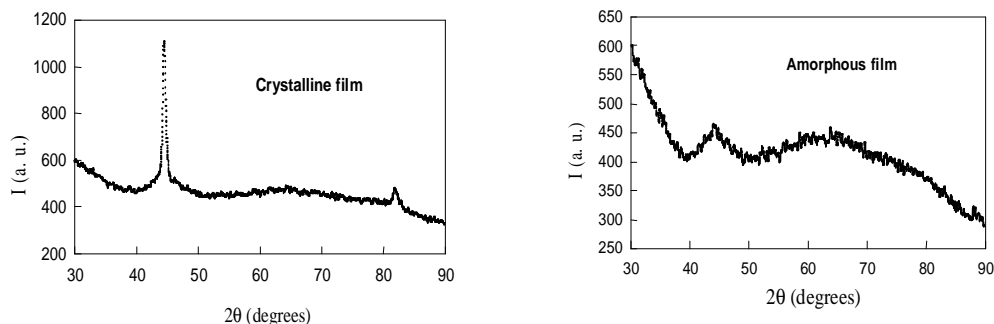


Fig. 3. X ray diffraction patterns of the METGLAS[®] films prepared with different pulse energy of the laser. Left 200 mJ per pulse (fluence 12.5 J/cm^2), right 80 mJ (fluence 5 J/cm^2).

The thickness of the samples ranged between 10 and 300 nm depending on the deposition conditions. The domain structure of selected samples was observed by the Bitter technique [22] using a commercial Ferroflid[®] EMG 607.

The coercive field, H_c , of the films prepared in the different regimes shows very different behaviour as a function of the thickness of the deposited samples. Under the first deposition conditions it increases monotonously with the deposition time, as the thickness does, but in the second set it shows a non-monotonous behaviour (Figs. 4 and 5).

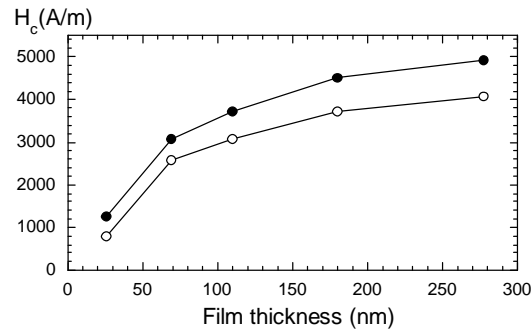


Fig. 4. Coercivity of the samples prepared under regime 1. Full symbols refer to as-prepared films, empty symbols are for annealed films. In the latter, internal stresses are relieved for half an hour at 350 °C annealing.

The shape of the hysteresis loops indicates the presence of in-plane anisotropy, which was traced to the surface properties of the substrate [20], but it decreases with the film thickness. Domain observation confirms the presence of in-plane magnetic anisotropy and shows that the different types of domain patterns correspond to films of different thickness prepared in the same regime being in agreement with usually observed behaviour [23]. Some domain walls in very thin films (30-50 nm) look like zigzag walls separating antiparallel domains. Increasing the thickness results in domain transformation into simple lancet type structures and an increase in the average domain size.

Fig. 5 shows the thickness and coercivity of the samples deposited in regime 2, as a function of the distance between the target and the lens [24]. The thickness increases as it approaches the focal point, and coercivity decreases from 2000 A/m at $d \approx 31,75$ cm down to very low value of about 400 A/m for samples deposited at 33.5 cm (almost focused beam). With films of low thickness, below 60 nm, the coercivity of the out of-focus samples is higher than that of the samples deposited in regime 1, but it is much lower for the high thickness values. Although additional study needs to be undertaken with smaller steps between focus-target distances, the value of 400 A/m, obtained here, is close to that reported for similar rf-sputtered soft amorphous films [9-10].

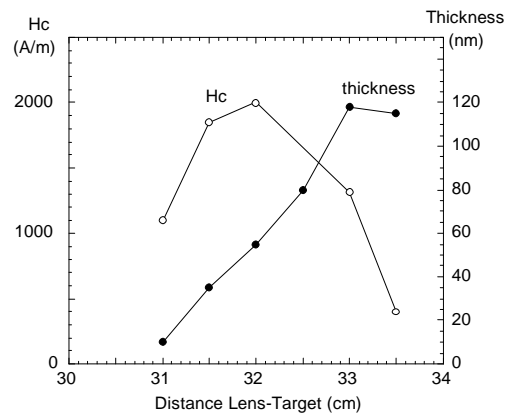


Fig. 5. Thickness and coercivity of the samples prepared under regime 2 as a function of the distance from the lens to the target. The best focus was obtained for $d = 33$ cm.

In conclusion, by changing the distance between the lens and the target, and using appropriate laser fluences, we were able to prepare very soft amorphous magnetostrictive thin films ($H_c \sim 400$ A/m) with very weak in-plane magnetic anisotropy. The coercivity achieved in these samples is appropriate for technological applications.

4. Granular magneto-resistive films

Granular alloys consisting in nanometer size grains of a ferromagnetic (FM) metal embedded into a noble metal matrix are known to display Giant Magneto-resistance (GMR) behaviour [25-27] similar to that of well defined metallic multi-layers alternating the same metals. However, the composition of the alloys has not a determinant role, except through the number, size and surface roughness of the clusters. Cluster size, on the other hand, determines the magnetic behaviour either as FM or super-paramagnetic (SPM).

Some $\text{Fe}_{30}\text{Ag}_{70}$ granular alloy's samples were produced in vacuum (10^{-5} mbar) using a mosaic type target. They were deposited onto glass substrates at room temperature and were about 500 nm thick. Laser fluency was about 15 Jcm^{-2} and target-substrate distance 4 cm. The differences between samples, arise from the frequency of the laser pulses (from 10 to 20 Hz) and rotation speed of the target (6 to 15 rpm). Both parameters can be merged in to a single one, which gives the number of laser pulses per revolution of the target. This parameter will be referred to as number of impacts per turn (ipt).

Fig. 6 shows the hysteresis loops as obtained by MOKE. The decrease of coercivity and remanence with the number of impacts per turn is clear. The samples with 100 and 150 ipt need a x5 magnification in order to be comparable to the low ipt ones.

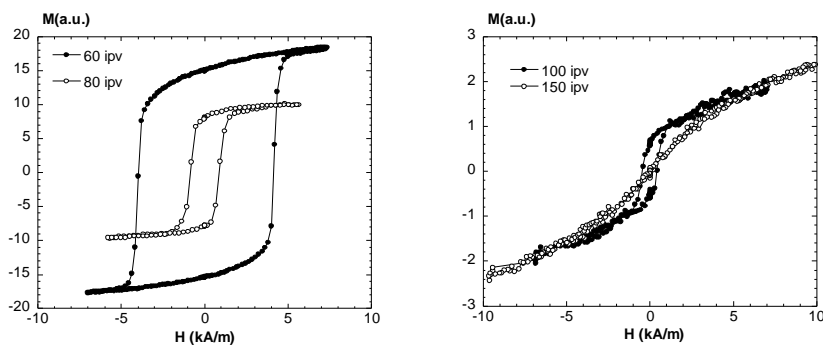


Fig. 6. Hysteresis loops of the samples with 60, 80, 100 and 150 impacts per turn (ipt). Complete absence of coercivity and remanence is shown for the 150 ipt sample.

These results can be interpreted in terms of the number and size of the Fe nanograins in the alloys. The size determine the FM or SPM behaviour of the grains, and only the number of grains above the SPM limit contribute to the hysteresis and coercivity [19,28]. If remanence and coercivity are taken as directly related to the number of FM Fe grains, the samples with high ipt should have very few or none of such FM grains or clusters. In such samples most of the iron should be in form of very small SPM clusters or directly dissolved in the silver matrix, acting as paramagnetic centres.

A direct observation of the number and size of the clusters can be performed by AFM. This technique is also easy to compare to the MOKE results as both give information of the surface of the sample. Topographic AFM images clearly show great differences between them regarding both the height and size of the surface protuberances. This clearly indicates a homogenisation of the sample surface as the number of ipt increases. The sample with 150 ipt is extremely flat and homogeneous, indicating an intimate mixing of the starting components. However, the lateral dimensions of the protuberances have no direct relation with the supposed size and distribution of the Fe grains in the Ag matrix. The size of the protuberances are extremely large (above 100nm) and do not follow a monotonous trend as a function of the number of ipt, or the corresponding magnetic properties of the samples.

The normal force feature of the AFM is expected to be sensitive to the local composition, as far as the differences between compositions are reflected in different elastic constants. This is the case here. As quoted by Kittel [29], the bulk modulus (and its inverse the compressibility) have very different values for Fe ($1.68 \times 10^{11} \text{ N/m}^2$) and Ag ($1.00 \times 10^{11} \text{ N/m}^2$). The 70% increase in modulus for iron allowed to discriminate the iron rich regions of the samples, as depicted in Fig. 7. The smallest visible contrast zones are about 5-10nm, i.e. at the resolution limit of the instrument.

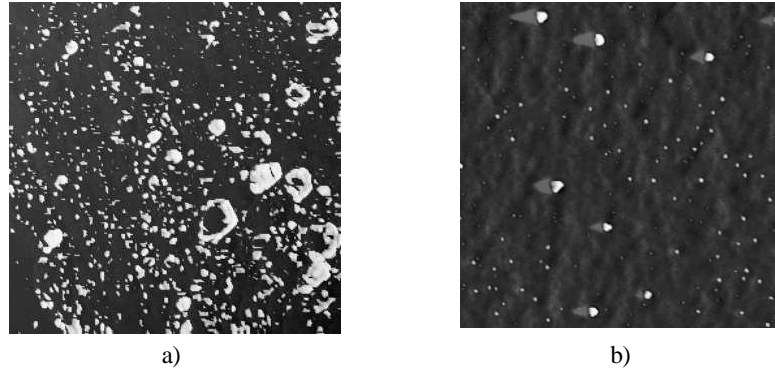


Fig. 7. Normal force AFM images of the samples with. a) 60, and b)100 ipt. Images have $1\mu\text{m} \times 1\mu\text{m}$ lateral size. Iron rich zones are clearly displayed as white spots.

Table 1. Characteristics of the granular Fe-Ag films (ipt = impacts per turn)

ipt	Hc (A/m)	Mr(relative)	Roughness(nm)	% Fe grains
60	4050	15	8	17
80	850	8	3	3
100	450	0.7	2.2	1
150	0	0	0.7	0

In conclusion, the normal force mode in AFM is able to discriminate the ferromagnetic iron nanograins in a silver matrix, and the results agree with, and provide a basis of explanation of the magnetic properties of the samples. The number and distribution of Fe grains are mainly determined by the number of laser impacts per turn of the mosaic target.

5. Oxide manganite films

Colossal magneto-resistance (CMR) mixed oxide films (manganites) are of great interest for technical applications. Their composition is $\text{Ln}_{1-x}\text{A}_x\text{MnO}_3$ (where Ln is a Lanthanide and A is a divalent cation) and they show the well-known perovskite structure. PLD is possibly the most popular technique for preparing films of these compounds, after the discovery of CMR in 1993 [30,31]. That was probably because of the large use of PLD for preparing High Tc superconductors with perovskite structure in the 80's. In addition epitaxial growth is observed when deposition takes place at the correct temperature onto single crystals of similar composition and lattice constant.

Among the different studied compositions the most effective as regarding applications is $\text{La}_{0.7}\text{Sr}_{0.3}\text{MnO}_3$ (LSMO). This compound presents the higher Curie temperature of the CMR perovskites and rather good values of the MR at room temperature. Therefore it is the most suitable for technical applications.

Six different kinds of samples were obtained using different target or deposition conditions, as summarised in Table 2. Targets prepared by the classical ceramic method or by softer chemical methods were tried. The substrates were either polycrystalline Alumina (Al_2O_3) or single crystals of LaAlO_3 (LAO). Another critical parameter is the oxygen partial pressure in the chamber. Two different values of this last parameter were chosen: 0.05 and 0.3 mbar.

Table 2. Deposition parameters and properties for the different LSMO films.

	Target	Substrate	O ₂ Pressure (mbar)	Tc(K)	MR (300K,1 Tesla)
SG- 03	Sol-gel	Al_2O_3 polycrystal	0.3	350	4%
SG- 005	" "	" "	0.05	180	≈2%
C- 03	Ceramic	" "	0.3	350	4.2%
C- 005	" "	" "	0.05	125	≈1%
Epi- 03	" "	LaAlO_3 (100)	0.3	270	8.5%
Epi- 005	" "	" "	0.05	70	≈1%

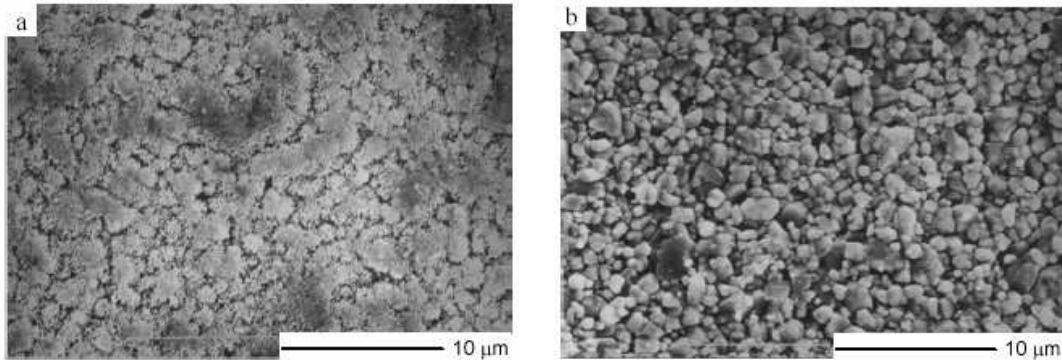


Fig. 8. SEM micrographies of the polycrystalline LaSrMnO films prepared under a) 0.3 mbar and b) 0.05 mbar of oxygen (Ceramic target).

SEM pictures of the polycrystalline samples show a granular structure having about $1\mu\text{m}$ grain size for the samples prepared with 0.05 mbar oxygen pressure, and several microns for the samples prepared with 0.3 mbar, irrespective of the target preparation method [15]. X ray diffraction shows large peaks indicative of the correct perovskite structure, with random crystallite orientations. Lattice parameters are $c=0.3860(3)$ nm for 0.3 mbar samples and $c=0.3885(3)$ for 0.05 mbar ones. Such differences can be attributed to oxygen deficiencies, as reported in the literature [32,33]. The line widths allow an estimation of the crystallite size, which is much lower than the grain size observed by SEM. Typical crystallite sizes are about 20 nm for 0.05 mbar samples and 45 nm for the 0.3 mbar samples.

Epitaxial samples are much more homogeneous but some droplets, about $1\mu\text{m}$ in diameter, are scattered all along the surface. Those droplets were probably also present in the polycrystalline samples but they were of the size of the grains so could not be distinguished from the overall texture of the films. X ray diffraction results show clearly the preferential 100 growth of the films as deduced from the presence of (n00) reflections exclusively. However the sample with low oxygen pressure presents double peaks for each index, indicating a double phase film. Phase A, corresponding to the high intensity peak, has a lattice constant $c=0.3870$ nm while the low intensity peak, phase B, has $c=0.400(3)$ nm. We can assume that the first layers, in contact with the substrate, are deformed due to the lattice mismatch (about 2.3 %) between the substrate (LAO) and film (LSMO). On the other hand, the other epitaxial film, prepared with 0.05 mbar is single phased, with $c=0.3901(3)$ nm. That can be due to the lattice distortion produced by the oxygen deficiency, which leads to a value close to that of the substrate.

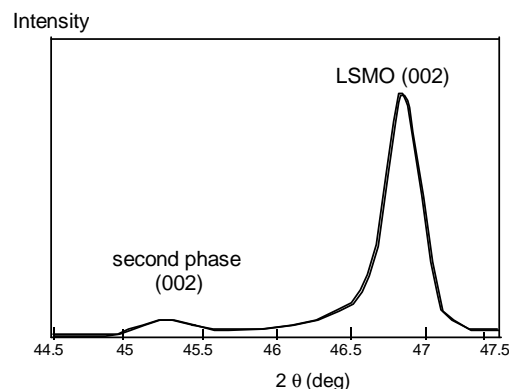


Fig. 9. (002) peak of the epitaxial 0.3 sample showing the existence of two phases.

Regarding the magnetic properties, the higher T_c values are obtained in polycrystalline films prepared under 0.3 mbar O_2 pressure: $T_c \approx 350$ K very close to that of the bulk material (363 K). Single crystal samples prepared with such O_2 pressure are of lower T_c (around 270 K). All samples

prepared with oxygen deficit (0.05 mbar) have much lower T_c (see Table 2), especially the epitaxial sample with the lowest T_c .

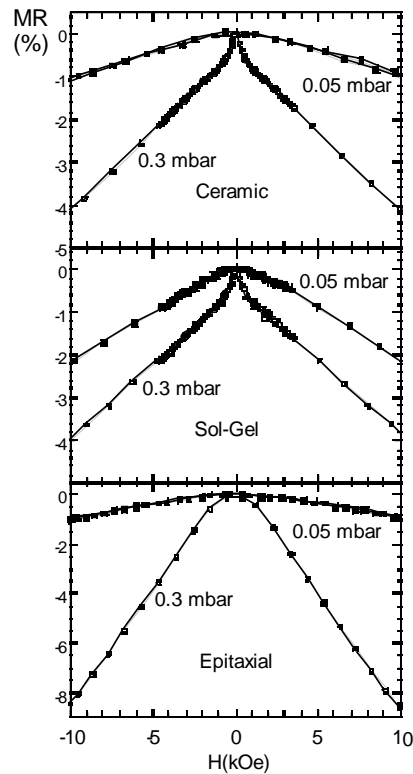


Fig. 10. Low field magnetoresistance of the different LSMO samples at room temperature. In all cases oxygen stoichiometry is fundamental for obtaining good properties.

The magnetoresistance of the films is large only in the proximity of the metal-insulating transition, close to T_c , so that only samples prepared with 0.3 mbar of oxygen are of some interest regarding applications, because of their T_c close or even above room temperature. Measurements in fields up to 60 kOe (6 Tesla) reveal maximum MR as large as 50% and even 65% at 10 K, higher than other values reported in the literature for similar composition films [34,35].

The room temperature and low field (10 kOe or 1 Tesla) MR is displayed in Fig. 10. We can see the minute MR effect in low oxygen samples (1-2%). In the polycrystalline films a very low field inter-grain contribution (about 0.7% at 1 kOe) is present for samples prepared at 0.3 mbar of oxygen. Such contribution is absent in the epitaxial film prepared with the same oxygen pressure. In that sample, the room temperature MR attains 9% in a field of 10 kOe, which is of great practical interest, but also in polycrystalline samples we found 4-5% values, enough for applications.

6. Conclusions

As shown, very different magnetic materials with clear technological applications can be prepared in form of thin films by means of Pulsed Laser Deposition techniques. The different compositions range from metallic amorphous films to single crystal magnetic oxides. The main preparation parameters influencing the properties of the films are pulse energy and repetition frequency, oxygen pressure and substrate temperature. In each case the influence of the parameters is different. For amorphous films the main parameter is the laser fluency. A secondary parameter is the laser focusing. The substrate nature is determinant for the in-plane anisotropy. In granular alloys, however, the number and size of the ferromagnetic grains is driven, mainly, by the number of impacts per unit time. The oxygen stoichiometry is a determinant factor in colossal magnetoresistant films. That parameter is easily controlled by changing the chamber partial oxygen pressure.

Other important parameter is the single crystal structure of the substrate, with a close lattice parameter to the oxide one, and the deposition temperature. In conclusion, by choosing the appropriate conditions and substrates, films of enough quality can be obtained, as to be used in technological applications for sensors or other applications.

Acknowledgements

We gratefully acknowledge Professor Hasegawa, of Honeywell, for supplying the METGLAS2605Co[®] ribbon, and Dr JS Garitaonandia for the help in the PLD set up. Dr. G.V. Kurlyandskaya acknowledges Prof. Blanca Hernando for the support during her stay at the Universidad de Oviedo. Most measurements were done by former PhD students: Ricardo López, Ana García, Pablo Mínguez and Alazne Peña. This work was partially supported by the Spanish Ministry of Science and Technology under grants MAT2001-0082 and MAT2002-04178 and by the Industry Department of the Autonomous Basque Government under the ACTIMAT project.

References

- [1] M. Tejedor, A. Fernández, *J. Magn. Magn. Mater.* **59**, 28 (1986).
- [2] E. Quandt, B. Gerlach, K. Seemann, *J. Appl. Phys.* **76**, 7000 (1994).
- [3] E. Rozenberg, D. Mogilanski, J. Pelleg, G. Gorodetsky, R. Somekh, *Thin Solid Films* **342**, 11 (1999).
- [4] A. V. Svalov, P. A. Savin, G. V. Kurlyandskaya, J. Gutiérrez, J. M. Barandiaran, V. O. Vas'kovskiy, *IEEE Trans. Magn.* **38**, 782 (2002).
- [5] A. García-Arribas, M. L. Fdez-Gubieda, J. M. Barandiaran, *J. Magn. Magn. Mater.* **196**, 164 (1999).
- [6] G. V. Kurlyandskaya, H. Yakabchuk, E. Kisker, N. G. Bebenin, H. García-Miquel, M. Vázquez, V. O. Vas'kovskiy, *Chin. Phys. Lett.* **18**, 1268 (2001).
- [7] Y. K. Kim, M. Oliveria, *J. Appl. Phys.* **74**, 1233 (1993).
- [8] D. Garcia, J. L. Muñoz, G. V. Kurlyandskaya, M. Vazquez, M. Ali, M. R. J. Gibbs, *J. Magn. Magn. Mater.* **191**, 339 (1999).
- [9] M. Ali, R. Watts, W. J. Karl, M. R. J. Gibbs, *J. Magn. Magn. Mater.* **190**, 199 (1998).
- [10] S. Q. Xiao, Y. H. Liu, S. S. Yan, Y. Y. Dai, L. Zhang, L. M. Mei, *Phys. Rev. B* **61**, 5734 (2000).
- [11] J. Wu, *Nanotechnology* **13**, 720 (2002).
- [12] A. Pérez-Junquera, J. I. Martín, M. Vélez, J. M. Alameda, J. L. Vicent, *Nanotechnology* **14**, 294 (2003).
- [13] P. I. Nikitin, A. A. Beloglazov, Yu. Toporov, M. V. Valeiko, V. I. Konov, A. Perrone, A. Luches, L. Mirengi, L. Tapfer, *J. Appl. Phys.* **82**, 1408 (1997).
- [14] K. Sturm, H. U. Krebs, *J. Appl. Phys.* **90**, 1061 (2001).
- [15] R. López Anton, J. J. Blanco, J. L. Muñoz, J. S. Garitaonandia, M. Insausti, A. Peña, T. Rojo, M. L. Fdez-Gubieda, J. M. Barandiarán, *Mater. Science Forum* **373-376**, 577 (2001).
- [16] S. W. Hwang, H. Y. Cheong, N. P. Ong, B. Batlogg, *Phys. Rev. Lett.*, **71**, 2041 (1996).
- [17] H. R. Khan, *Mater. Science Forum* **373-376**, 93 (2001).
- [18] Z. Q. Qiu, S. D. Bader, *J. Magn. Magn. Mater.* **200**, 664 (1999).
- [19] B. D. Cullity, *Introduction to Magnetic Materials*, Addison-Wesley, Reading, MA, 1972.
- [20] J. M. Barandiarán, P. Mínguez, G. V. Kurlyandskaya, *J. Non-Cryst. Solids.*, in press.
- [21] T. Meydan, P. I. Williams, A. N. Grigorenko, P. I. Nikitin, A. Perrone, A. Zocco, *Sensors and Actuators A81*, 254 (2000).
- [22] F. Bitter, *Phys. Rev.* **41**, 507 (1932).
- [23] A. Hubert, S. Schäfer, *Magnetic Domains. The Analysis of Magnetic Microstructures*, Springer-Verlag, 1998.
- [24] G. V. Kurlyandskaya, J. M. Barandiarán, P. Mínguez, L. Elbaile, *Nanotechnology* **14**, 1 (2003).

-
- [25] A. E. Berkowitz, J. R. Mitchell, M. J. Carey, A. P. Young, S. Zhang, F. E. Spada, F. T. Parker, A. Hutten, G. Thomas, *Phys. Rev. Lett.* **68**, 3745 (1992).
- [26] J. Q. Xiao, J. S. Jiang, C. L. Chien, *Phys. Rev. Lett.* **68**, 3749 (1992).
- [27] M. N. Baibich, J. M. Broto, A. Fert, F. Nguyen Van Dau, F. Petroff, P. Etienne, G. Creuzet, A. Friederich, J. Chazeles, *Phys. Rev. Lett.* **61**, 2472 (1988).
- [28] S. Chikazumi, *Physics of Magnetism*, R.E. Krieger Pub. Co., New York, 1978.
- [29] C. Kittel, *Introduction to Solid State Physics*, John Wiley & Sons, New York, 1971.
- [30] S. Jin, T.H. Teifel, M. McCormack, R.A. Fastnacht, R. Ramesh, L.H. Chen, *Science* **264**, 413 (1993).
- [31] R. von Helmolt, J. Wecker, B. Hopzapfel, L. Schultz, K. Samwer, *Phys. Rev. Lett.* **71**, 2331 (1993).
- [32] M. Rajeswari, M. Shreekala, A. Goyal, S. E. Lofland, S. M. Bhagat, K. Ghosh, R. P. Sharma, R. L. Greene, R. Ramesh, T. Venkatesen, T. Boettcher, *Appl. Phys. Lett.* **73**, 2672 (1998).
- [33] H. L. Ju, J. Gopalakrishnan., J. L. Peng, Q. Li, G. C. Xiong, T. Venkatesan, R. L. Greene, *Phys. Rev. B* **51**, 6143 (1995).
- [34] R. von Helmolt, J. Wecker, K. Samwer, L. Haupt, K. Bärner, *J. Appl. Phys.* **76**, 6925 (1994).
- [35] W. Zhang, I. W. Boyd, N. S. Cohen, Q. T. Bui, Q. T. Pankhaurst, *Appl. Surface Sci.* **110**, 350 (1996).